ACS APPLIED MATERIALS & INTERFACES

Research Article

www.acsami.org

Nanocomplex Based on Biocompatible Phospholipids and Albumin for Long-Circulation Applications

Qiang Peng,[†,§] Xue-Qin Wei,[†,§] Xiao-Ru Shao,[†] Ting Zhang,[‡] Shu Zhang,[†] Na Fu,[†] Xiao-Xiao Cai,[†] Zhi-Rong Zhang,[‡] and Yun-Feng Lin*[,†]

[†]State Key Laboratory of Oral Diseases, West China Hospital of Stomatology, Sichuan University, Chengdu 610041, China

[‡]Key Laboratory of Drug Targeting and Drug Delivery Systems, Ministry of Education, West China School of Pharmacy, Sichuan University, Chengdu 610041, China

ABSTRACT: Achieving long circulating delivery of nanoparticles (NPs) is important for efficient drug therapy, but it is difficult due largely to proteins adsorption (opsonization) or/and nonsufficient stability of NPs. In this present work, we aimed to address the above issues by constructing a phospholipid and BSA-based nanocomplex system, namely BSA−phospholipid NPs (BSA-PL-NPs). Combining sodium dodecyl sulfate-polyacrylamide gel electrophoresis, X-ray photoelectron spectroscopy and proteins adsorption property, we confirmed that some BSA molecules were fixed on the inner surface of BSA-PL-NPs via hydrophobic interactions and the others were located in the core area. This special configuration allowed BSA-PL-NPs to not only maintain the antiadsorption and low phagocytosis properties but also have the slow zero-order drug release and the enhanced nanostructure stability. Interestingly, we found that BSA-PL-NPs had no cytotoxicity to mouse L929 fibroblasts but could stimulate the cells' growth instead. In conclusion, BSA-PL-NPs have a great potential to be developed as a long-circulation drug delivery system, and the ready availability, biocompatibility and nontoxicity of phospholipids and albumin give this system great promise for practical use.

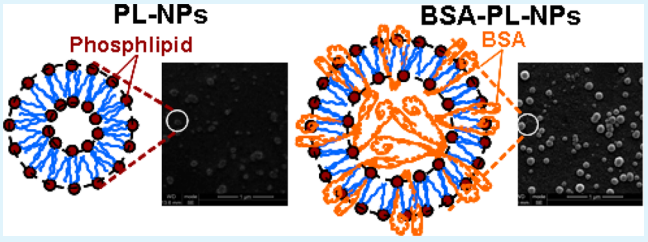

KEYWORDS: *nanoparticles, long circulation, drug delivery, proteins adsorption, toxicity, stability*

INTRODUCTION

In the past few decades, nanoparticles have attracted worldwide attention due basically to their particular properties, like their nanoscale size and large surface area. That is, these properties give nanoparticles quite different behaviors compared to their bulk materials.[1−3] With the rapid development of nanotechnology, the great potential of nanoparticles in biomedicine and drug delivery has also been explored. It has been found that encapsulating drugs into nanoparticles is an effective approach to enhance drug solubility and bioavailability.[4−6] In addition, nanoparticles are used as an important carrier for targeting delivery of therapeutic molecules.[6−10] Despite the wide applications of nanoparticles, their short circulating time in the bloodstream after intravenous administration is a big problem for further development and practical use. Lots of reasons can result in such a problem, among which, rapid uptake by the mononuclear phagocyte system and intrinsic instability of the nanoparticles contribute a lot to the short circulation.

It is well-known that nanoparticles will be covered with plasma proteins immediately after their entry into the blood.[11−15] These spontaneously formed proteins corona becomes the material that organs and cells really "see", and thus changes the in vivo fate of nanoparticles.[16,17] One of the most undesired changes is the rapid clearance of nanoparticles from the blood due to the adsorption of opsonins after intravenous injection. To avoid or reduce the formation of proteins corona and to achieve long circulation, polyethylene glycol (PEG)ylation is commonly used to improve the surface properties of nanoparticles. Although progress is made, the results vary in different reports.[18−21] In addition, the reproducibility of PEGylation is relatively low, leading to a less possibility for practical use. Therefore, searching for a material that is readily available and possesses the similar effect to PEGylation may be an approach to address the above issue.

Phospholipids, an important surfactant in our body, have a hydrophilicity property similar to PEG. Most importantly, they are the main composition component in the cell membrane, indicating their safety as well as possibility for use as a carrier. Their intrinsic antiadhesion properties can inhibit the formation of proteins corona.[22−24] In addition, our previous works have demonstrated their ability to encapsulate drug molecules in the form of nanoparticles.[25,26] Theoretically, phospholipids could be an ideal material for fabrication of long-circulation nanoparticles. However, their fast drug release and short blood half-life indicate that the stability of phospholipids nanoparticles is too low to enable long-term circulation in the bloodstream.[22,26,27] Therefore, a proper stabilizer is needed to prepare long-circulation phospholipids based nanoparticles.

Received: May 22, 2014
Accepted: July 24, 2014
Published: July 24, 2014

Albumin, the most abundant protein in plasma, has lots of important functions, like maintaining plasma osmotic pressure and detoxification. It has been developed as a carrier to deliver various drugs due to its nontoxicity, ready availability and long half-life.[28] In our previous work, we have demonstrated the protective effect of albumin coating on hydrophobic polymeric nanoparticles.[13] According to the configuration, the hydrophobic domain of albumin can interact with the hydrophobic part of other molecules, like the fatty acid tail of phospholipids. Thus, albumin may be a potential stabilizer for phospholipids nanoparticles. It is noticeable that both phospholipids and albumin are approved materials for pharmaceutical use, implying that the nanocomplex based on them has a great potential for practical use in the future.

Therefore, in this present work, we aim to use BSA as a functional stabilizer to develop a nanocomplex system consisting of BSA and phospholipids (BSA-PL-NPs), whose special configuration is disclosed for the first time (Scheme 1).

Scheme 1. Schematics of Structure Difference between PL-NPs and BSA-PL-NPs[a]

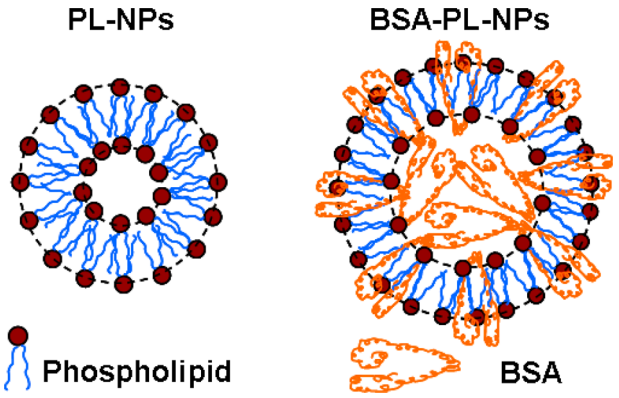

[a]PL-NPs are smaller in size and their structure is instable. In the presence of BSA, some BSA molecules are fixed on the inner surface of BSA-PL-NPs and the others are incorporated in the inner space, leading to the larger size and higher stability.

We also investigate the protective effect of BSA on phospholipid-based nanoparticles, and evaluate the potential of BSA-PL-NPs for developed as long circulating nanoformulations.

EXPERIMENTAL SECTION

Materials. Phospholipids (soybean lecithin for injection use, with phosphatidylcholine content higher than 70%) was purchased from Shanghai Tai-Wei Pharmaceutical Co. Ltd. (Shanghai, China). Bovine serum albumin (BSA) was purchased from Amresco (Solon, OH, USA). Fetal bovine serum (FBS) was purchased from HyClone (Logan, UT, USA). Coumarin-6 (C6) was purchased from Sigma (St. Louis, MO, USA). All other chemical reagents used in this study were of analytical grade or better.

Animals. The healthy male Kunming mice (20−25 g) were purchased from Experimental Animal Centre of Sichuan University (Chengdu, China). All the animal experiments were approved by the Institutional Animal Care and Ethic Committee of Sichuan University. The mice were housed in cages (10 mice per cage) under controlled conditions (~25 °C, ~55% air humidity) with free access to food and tap water.

Preparation of Original Phospholipids Nanoparticles (PL-NPs) and BSA−Phospholipids Nanoparticles (BSA-PL-NPs). The PL-NPs were prepared according to the previous method with some modifications.[26] Briefly, the weighed phospholipid was dissolved in absolute ethanol serving as the organic phase. Under rapid magnetic stirring, the resulting organic solution was injected into distilled water at a volume ratio of 1:10, followed by sonication for five times at the power of 20%. The PL-NPs suspension was obtained after evaporation at 45 °C for 20 min. When BSA-PL-NPs was prepared, the distilled water was replaced by 20 mg/mL BSA solution and the other procedures were the same as above. The coumarin-6 loaded NPs (C6-PL-NPs and C6-BSA-PL-NPs) were prepared by codissolving C6 and phospholipid in ethanol followed with the same other procedures as above.

Characterization of PL-NPs and BSA-PL-NPs. The particle size, size distribution and ζ-potential of nanoparticles were measured by dynamic light scattering (DLS) and electrophoretic light scattering (ELS) technologies, respectively, using the instrument of Zetasizer Nano ZS90 (Malvern Instruments Ltd., Malvern, U.K.). The particle size was presented by intensity distribution, and polydispersity index (PDI) was used to evaluate the size distribution. The morphology of nanoparticles was observed by scanning electron microscopy (SEM, INSPECT F, FEI, Eindhoven, The Netherlands). One drop of the properly diluted nanoparticles suspension was placed on a clean glass sheet, followed by air-drying. The samples were coated with gold before SEM.

Interaction of NPs with Proteins. The protein adsorption properties of PL-NPs and BSA-PL-NPs were investigated using BSA as a representative protein or diluted mouse serum. Briefly, the freshly prepared PL-NPs were mixed with BSA solution (20 mg/mL) and incubated for 2 h at room temperature, and the freshly prepared BSA-PL-NPs were stilly placed because it was already in the BSA solution. Meanwhile, PL-NPs and BSA-PL-NPs were incubated with 5-fold diluted mouse serum, followed with size measurement at fixed time intervals. In addition, the adsorption ratio of BSA was also determined. Briefly, after incubation with BSA for 2 h, the resultant suspension was filtered through membranes (0.22 μm). The initial drops of filtrate that may contain very small size nanoparticles were discarded and the later filtrate was collected and properly diluted for free BSA (Ff) content determination by fluorescent spectrometry (excitation, 280 nm; emission, 332 nm). The total BSA (Ft) content was quantified in the same manner. The nonadsorption ratio can thus be calculated by Ff/Ft.

Sodium Dodecyl Sulfate-Polyacrylamide Gel Electrophoresis (SDS-PAGE) of PL-NPs and BSA-PL-NPs. To confirm the existence of BSA in the BSA-PL-NPs, 12% SDS-PAGE was used to separate the associated BSA. The BSA-PL-NPs were separated by centrifugation (16 krcf, 5 min) and washed three times to get rid of free BSA. Then, PL-NPs and the treated BSA-PL-NPs were subjected to 12% SDS-PAGE.[13]

X-ray Photoelectron Spectroscopy (XPS). To estimate the location of BSA in BSA-PL-NPs, surface element analysis was performed using XPS. Briefly, PL-NPs and BSA-PL-NPs were condensed by filtering through a microporous membrane, respectively. The BSA-PL-NPs were washed with large quantity of water to remove the free BSA. After naturally drying, the chemical elements carbon (C), nitrogen (N), oxygen (O) and phosphorus (P) of these samples were analyzed using XPS.

In Vitro Release Study. The NPs stability also influences the drug release. Therefore, the in vitro release property of C6-PL-NPs and C6-BSA-PL-NPs was investigated using the dynamic dialysis method.[4] Briefly, 1 mL of C6-PL-NPs or C6-BSA-PL-NPs was added into a dialysis bag. After tightly bundled at two ends, the sample loaded dialysis bags were soaked in 8 mL of release medium (PBS containing 0.5% (m/v) of the Tween 80, pH 7.4) and placed on a horizontal shaker (70 rpm, 37 ± 1 °C). At fixed time intervals, the release medium was collected and replaced with 8 mL of fresh medium. The collected samples were stored at −80 °C for further analysis by fluorescent spectrophotometry (excitation, 464 nm; emission, 502 nm).

Accelerated Stability of PL-NPs and BSA-PL-NPs. The accelerated stability was conducted under high speed centrifugation, and C6 loaded NPs (C6-PL-NPs and C6-BSA-PL-NPs) were involved

Table 1. Size and ζ-Potential Test of PL-NPs and BSA-PL-NPs[a]

samples	size (nm)	PDI	ζ-potential (mv)	pH
PL-NPs	160.5 ± 3.5	0.389 ± 0.043	−35.6 ± 1.9	6.71 ± 0.05
BSA-PL-NPs	184.9 ± 2.8[b]	0.289 ± 0.025[c]	−11.8 ± 0.2[d]	6.98 ± 0.09

[a]Data are presented as mean ± s.d. (n = 3). Significant difference between NPs and NPs-BSA. [b]$P < 0.001$. [c]$P < 0.05$. [d]$P < 0.01$.

in this experiment. Briefly, C6-PL-NPs and C6-BSA-PL-NPs were centrifuged at 16 krpm for 10 min. The supernatant (0.5 mL) was taken and diluted to 5 mL with dimethyl sulfoxide (DMSO), and the leaked C6 was quantified by fluorescent spectrophotometry (excitation, 464 nm; emission, 502 nm). Similarly, 0.5 mL of the NPs suspension before centrifugation was diluted to 5 mL with DMSO and the total C6 content was measured. The stability (S) was then calculated using the following equation: $S = (A_1 - A_0)/A_0 \times 100\%$, where A_0 and A_1 were the fluorescent intensity before and after centrifugation, respectively.

In Vitro Metabolic Stability in Liver Homogenate. To find out the impact of BSA on the stability of PL-NPs under physiological environment, we investigated the in vitro metabolic stability of PL-NPs and BSA-PL-NPs in mouse liver homogenate that was prepared based on a previous report.[29] First, the liver was separated from the sacrificed mice and washed with cold water to get rid of the blood on the surface. Subsequently, the liver was mixed with cold PBS (containing 100 × 10 000 U/mL penicillin G sodium, 10 000 mg/mL streptomycin sulfate and 25 mg/mL amphotericin B as fungizone, pH 7.4) at the weight ratio of 1:5 followed by homogenization. After centrifugation at 4 °C (12 krpm, 10 min), the supernatant was used immediately or stored at −80 °C for further use.

The C6-PL-NPs or C6-BSA-PL-NPs with equal content of C6 were dispersed in 0.2 mL liver homogenate prepared above followed by incubation at 37 °C with shaking at 100 rpm. At fixed time intervals, the C6 remained was extracted with a mixed solvent (methanol:ethyl acetate = 1:1) twice. The organic solution was collected and dried by air-flow at 37 °C and the residue was reconstituted in methanol by vortex. After centrifugation, the supernatant (50 μL) was injected into a high performance liquid chromatography (HPLC) system with a fluorescent detector (excitation, 464 nm; emission, 502 nm). The C6 content was determined with an internal standard method, in which coumarin-7 served as the internal standard.

In Vitro Phagocytosis by Raw264.7 Cells. The C6-PL-NPs and C6-BSA-PL-NPs were also involved in this experiment. Briefly, the mouse macrophages (Raw264.7) were supplied with RPMI-1640 culture medium containing 10% FBS and cultured under standard conditions (37 °C, 5% CO_2). Then, the cells suspension (50 000 cells/ml) was prepared, 1 mL of which was mixed with 0.5 mL of the diluted NPs in centrifuge tubes. The final C6 concentration in the resultant mixture was 0.3125, 0.625, 1.25 or 2.5 μg/mL. After incubation at 37 °C for 1 h, the free NPs were separated from cells by centrifugation (3000 rpm, 3 min), and the C6 content in the supernatant was measured by fluorescent spectrophotometry after proper dilution (excitation, 464 nm; emission, 502 nm). The phagocytosed amount of NPs was therefore calculated by the C6 content difference between the total C6 amount and the free C6 amount. In addition, the cells were resuspended and subjected to fluorescent microscopy to observe the fluorescent signal in cells.

In Vitro Cytotoxicity. The cytotoxicity of PL-NPs and BSA-PL-NPs were evaluated using the real-time cell analysis system (RTCA, xCELLigence DP).[30,31] The proliferation of mouse L929 fibroblasts was examined. Briefly, the cells were plated onto the specially made 16-well cell culture plates (Eplate 16) at a density of 10 000 cells per well and cultured at 37 °C/5% CO_2 for 24 h in RPMI-1640 culture medium containing 10% fetal bovine serum (FBS). Then, the culture medium was replaced with PL-NPs or BSA-PL-NPs contained medium that contained no FBS (four particle concentrations were involved: 112.5, 225, 450 and 900 μg/mL). Cell proliferation, before and after exposure to nanoparticles, was recorded by RTCA system.

Statistical Analysis. In this present work, all the data are presented as mean ± s.d. (standard deviation). The one-way analysis of variance was used to compare the difference between groups, which was considered to be statistically significant when the p-value was less than 0.05.

RESULTS AND DISCUSSION

Characterization of PL-NPs and BSA-PL-NPs. As shown in Table 1, the size of BSA-PL-NPs is about 185 nm, significantly larger than that of PL-NPs ($P < 0.001$). There are two possibilities for the larger size: one is from the BSA layer adsorbed around the NPs surface; on the other hand, BSA is incorporated in the inner space of NPs, making these particles a little bloated. In addition to particle size, the polydispersity index (PDI) is another important parameter to evaluate NPs, which is the lower the better. In this work, BSA-PL-NPs have a significantly lower PDI than PL-NPs ($P < 0.05$), indicating that the size distribution of BSA-PL-NPs is more narrow. In another word, BSA-PL-NPs are more homogeneous in size (Figure 1AB). More interestingly, the ζ-potential of BSA-PL-NPs is much smaller than that of PL-NPs ($P < 0.01$, Table 1 and Figure 1CD). It is assumed that some of the incorporated BSA molecules, which are negatively charged, interact with the hydrophobic tail of phospholipids by a hydrophobic effect.

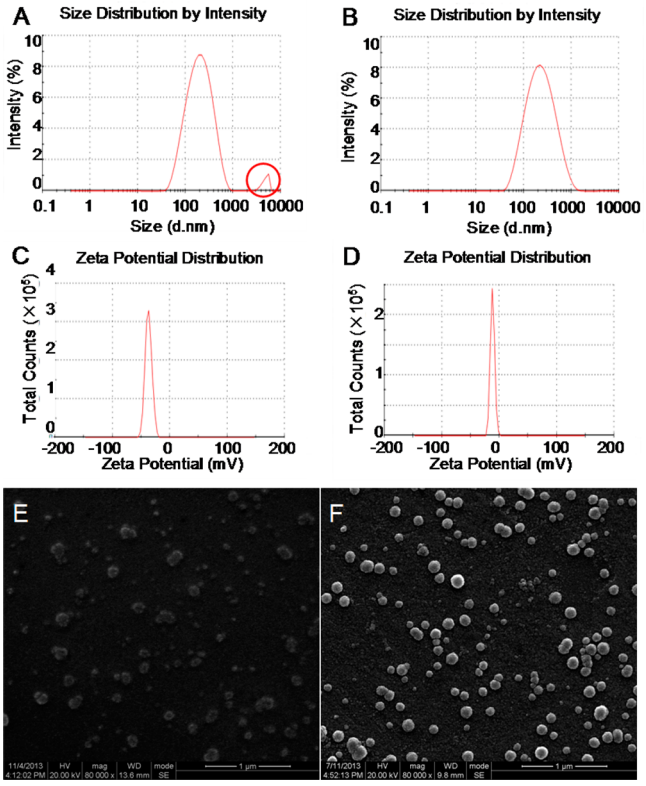

Figure 1. Characterization of PL-NPs and BSA-PL-NPs. (A, B) Typical size distribution of PL-NPs and BSA-PL-NPs, respectively. (C, D) Typical ζ-potential distribution of PL-NPs (pH 6.75) and BSA-PL-NPs (pH 6.90), respectively. (E, F) SEM images of PL-NPs and BSA-PL-NPs, respectively (scale bar: 1 μm).

These negatively charged BSA molecules are therefore fixed on the inner surface of NPs (Scheme 1), leading to a lower potential difference.

The morphology of NPs was observed by SEM. As shown in Figure 1E, PL-NPs look flat in appearance, and some particles are large in size but some of the others are too small, indicating that the size distribution of PL-NPs is not regular. In contrast, BSA-PL-NPs are spherical in shape and the particle size is more homogeneous (Figure 1F). These results are fully consistent with the PDI values (Table 1) and the size distribution graphs (Figure 1AB).

Interaction of NPs with Proteins. It is known that the intrinsic antiadhesion properties of phospholipid can inhibit the proteins adsorption.[22−24] In this experiment, we tested the protein adsorption properties of PL-NPs and BSA-PL-NPs using BSA as well as diluted mouse serum. As expected, neither PL-NPs nor BSA-PL-NPs have substantial change in size after incubation with BSA (Figure 2A) for 2 h or with mouse serum

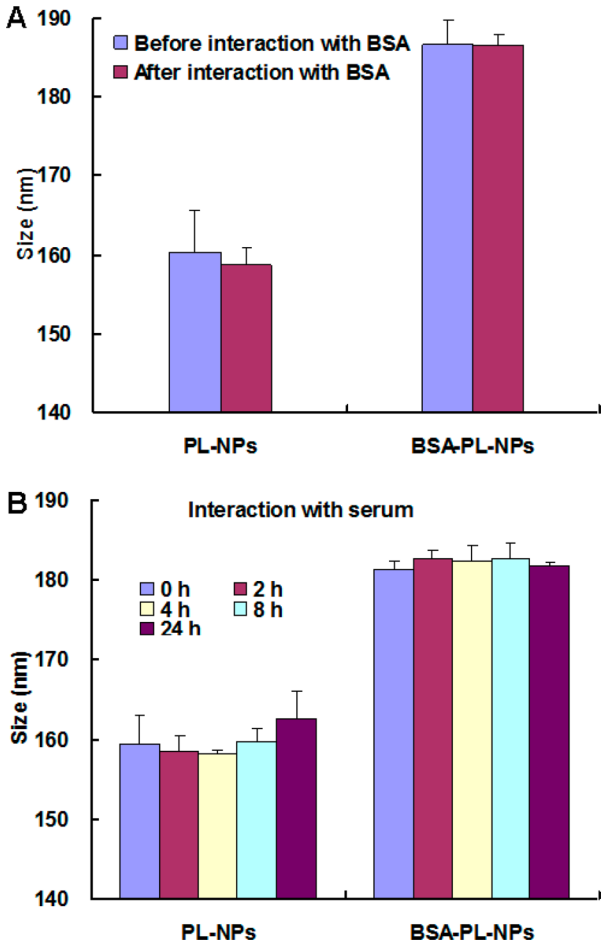

Figure 2. Interaction of PL-NPs and BSA-PL-NPs with proteins. (A) Size change after incubation with BSA (20 mg/mL) for 2 h. (B) Size change after incubation with mouse serum (5-fold diluted) within 24 h. Data are presented as mean ± s.d. (n = 3).

for a period of 24 h (Figure 2B). In addition, the BSA nonadsorption ratio for PL-NPs and BSA-PL-NPs was 99.07 ± 0.06% and 98.75 ± 0.02%, respectively. These results suggest that the incorporated BSA has no influence on the antiadhesion properties of PL-NPs and that BSA-PL-NPs maintain the antiprotein adsorption properties. Therefore, the larger size of BSA-PL-NPs (Table 1) is likely attributed to the BSA incorporated in NPs rather than the BSA adsorbed on the outer surface of NPs.

Confirmation and Localization of BSA in BSA-PL-NPs. 12% SDS-PAGE and XPS were used for confirmation and localization of BSA in BSA-PL-NPs, respectively. As shown in Figure 3A, there is no protein band for PL-NPs, whereas an

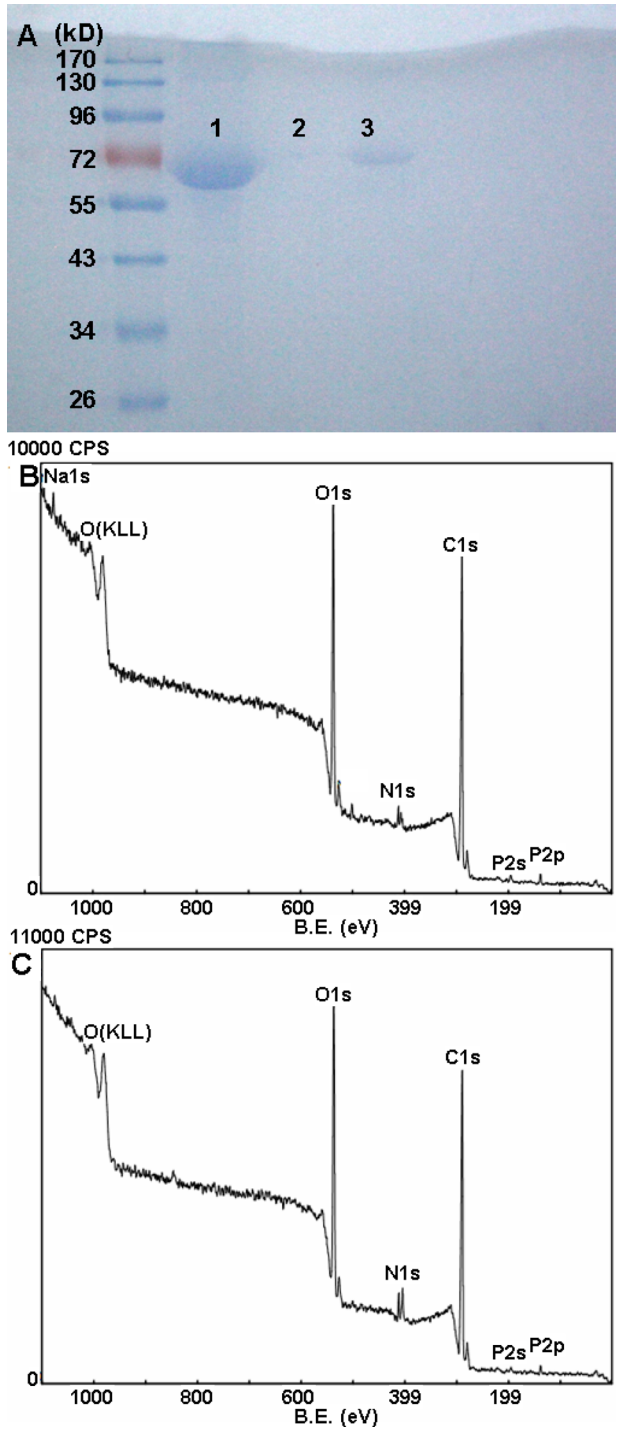

Figure 3. Confirmation and localization of BSA in BSA-PL-NPs. (A) 12% SDS-PAGE and Coomassie Brilliant Blue staining of BSA (line 1, BSA standards; line 2, PL-NPs; line 3, BSA-PL-NPs) (B, C) XPS graphs of surface element analysis for PL-NPs and BSA-PL-NPs, respectively.

dx.doi.org/10.1021/am503179a | ACS Appl. Mater. Interfaces 2014, 6, 13730−13737

obvious BSA band is observed for BSA-PL-NPs, indicating the existence of BSA in BSA-PL-NPs. SDS-PAGE can only confirm the existence of BSA, whereas XPS can help us confirm the location of BSA due to its ability of surface chemical elements analysis. Element signals for C, N, O and P can be found in both PL-NPs and BSA-PL-NPs but the intensity of the same element varies (Figure 3BC). The detailed elements analysis is shown in Table 2. It is interesting to find that the surface

Table 2. XPS Analysis of Surface Elements of PL-NPs and BSA-PL-NPs

	elements content (%)			
samples	C	N	O	P
PL-NPs	68.39	4.58	25.74	1.29
BSA-PL-NPs	65.61	6.63	26.85	0.90

elements content of PL-NPs is substantially different with that of BSA-PL-NPs. Particularly, the content of elements N and O increases while the content of C and P decreases in BSA-PL-NPs. Such changes are undoubtedly resulted from BSA that contains a large amount of N and O. In another word, BSA should be located near the surface of BSA-PL-NPs. We have demonstrated above (Figure 2A) that BSA is not adsorbed on the outer surface of BSA-PL-NPs. Hence, BSA molecules should be fixed on the inner surface of BSA-PL-NPs (Scheme 1) so that they can be detected by XPS, which supports the explanation for the lower ζ-potential of BSA-PL-NPs (Table 1).

In Vitro Release Study. Drug release from NPs is an important parameter to evaluate the NPs based drug delivery system. The release behavior of BSA-PL-NPs may be influenced due to the presence of BSA compared with PL-NPs. As shown in Figure 4, the release speed of C6-BSA-PL-NPs is significantly slower than that of C6-PL-NPs, which is probably due to (a) the block-like effect of the incorporated BSA and (b) the higher skeleton stability of BSA-PL-NPs. There are three approaches for drug release from NPs: (a) the drug molecules adsorbed on the surface of NPs are released via desorption upon contacting with release medium, (b) the

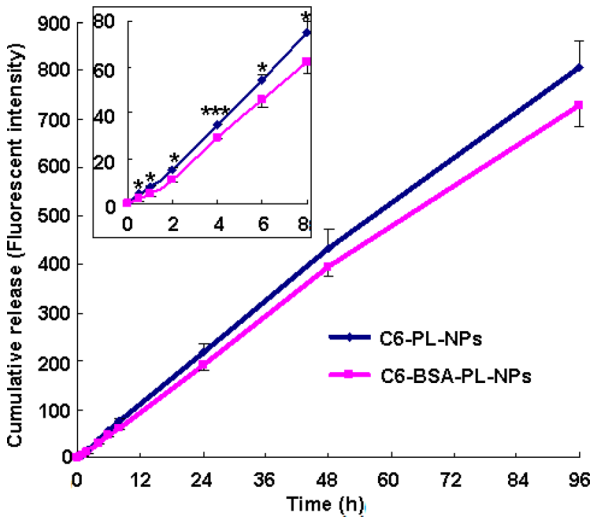

Figure 4. In vitro release profiles of C6-PL-NPs and C6-BSA-PL-NPs in PBS containing 0.5% (m/v) of the Tween 80 (pH 7.4). Insert is the magnification of release profiles within the first 8 h. Data are presented as mean ± s.d. (n = 3). *P < 0.05, ***P < 0.001.

encapsulated drugs are released by diffusion through the NPs skeleton or/and (c) following the degradation or disintegration of NPs.[4] In this present work, the incorporated BSA molecules may act as barriers blocking the diffusion of C6. In addition, the potential interaction of coumarins with BSA may also contribute to the slower release of C6-BSA-PL-NPs.[32] Meanwhile, the possible higher stability of BSA-PL-NPs may slow C6 diffusion. From Figure 4 we can also see that neither C6-PL-NPs nor C6-BSA-PL-NPs have initial burst release which is the common phenomenon for lots of NPs systems.[33,34] Furthermore, the release profiles of both C6-PL-NPs and C6-BSA-PL-NPs are quite close to zero-order release kinetics. In another word, the release speed is nearly constant, which is the feature of controlled release systems and can be achieved in a very few NPs based drug delivery systems.[35,36]

Accelerated Stability and Metabolic Stability in Vitro. The leakage of the loaded drug is one of the defects of NPs based drug delivery systems, which is tightly related to NPs stability. The disintegration of the NPs framework will be accelerated under imposed forces. Here we examined the accelerated stability of C6-PL-NPs and C6-BSA-PL-NPs under high speed centrifugation. As shown in Figure 5A, the

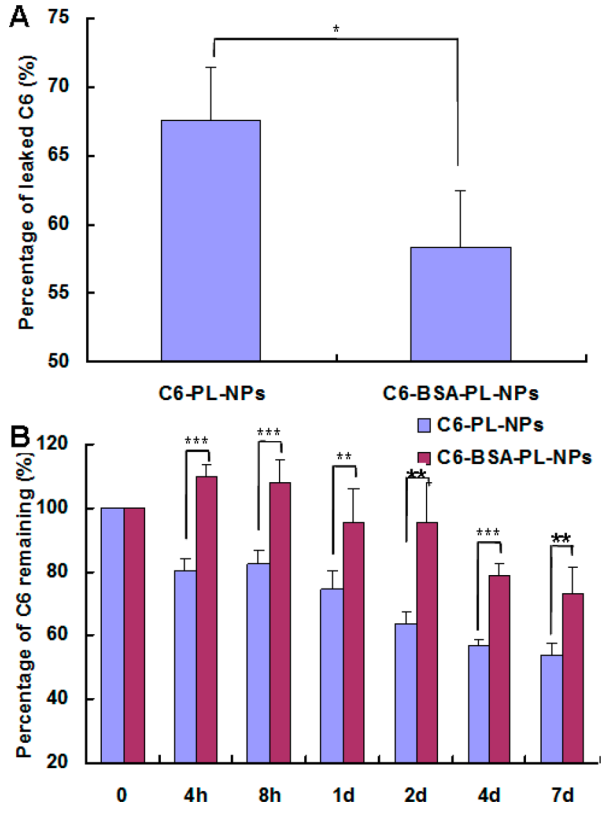

Figure 5. In vitro stability of C6-PL-NPs and C6-BSA-PL-NPs under different conditions. (A) Accelerated stability at high speed centrifugation (16 krpm, 10 min). (B) Metabolic stability in mouse liver homogenate. Data are presented as mean ± s.d. (n = 5). *P < 0.05, **P < 0.01, ***P < 0.001.

percentage of leaked C6 is about 68% for C6-PL-NPs, significantly higher than that for C6-BSA-PL-NPs (~58%, P < 0.05), suggesting the higher stability of C6-BSA-PL-NPs. It is undoubted the incorporated BSA plays an important role in reinforcing the NPs structure (Scheme 1). First of all, the BSA fixed on the inner surface may function as sponge-like buffers,

weakening the forces from centrifugation. In addition, the BSA existing in the inner space may play as both buffers and fillers reducing the compression space and thus supporting NPs against collapse.

The stability of NPs in organs will influence their metabolic speed and the elimination rate of a drug. Among the organs, the liver is the most important one. Here we examined the metabolic stability of C6-PL-NPs and C6-BSA-PL-NPs in mouse liver homogenate. The C6 content remaining after incubation with liver homogenate was quantified to indicate the stability. As shown in Figure 5B, only ~80% C6 remains after 8 h for C6-PL-NPs whereas almost no C6 is metabolized during the same time for C6-BSA-PL-NPs ($P < 0.001$). The C6 content of C6-BSA-PL-NPs decreases to 80% until 4 d, when, in contrast, only ~56% of C6 is intact for C6-PL-NPs ($P < 0.001$). Furthermore, the C6 content of C6-BSA-PL-NPs is always over 70% throughout the experiment (~73% at 7 d). These results imply that BSA-PL-NPs have a significantly higher metabolic stability than PL-NPs. In combination with other results shown above, there are at least three reasons for the higher metabolic stability of BSA-PL-NPs: (a) the slower release property of BSA-PL-NPs (Figure 4) reduces the amount of loaded drug exposed to the liver homogenate in the outer area of NPs, (b) the solid skeleton of BSA-PL-NPs (Figure 5A) is helpful to resist the metabolic effect and (c) the BSA fixed on the inner surface of BSA-PL-NPs also functions as a barrier for the metabolic enzymes contained in the liver homogenate, restricting their entry into the inner space of NPs and thus reducing the amount of metabolic enzymes to which the loaded drug is exposed.

In Vitro Phagocytosis by Raw264.7 Cells. Cell uptake, associated with the properties of material, has a significant impact on the fate of NPs in a biological environment.[37,38] Recognition and phagocytosis by macrophages is an important approach for the body to clear the exogenous particles including NPs. Therefore, phagocytosis rate has a substantial impact on the circulation time of NPs. Here we investigated the phagocytosis of C6-PL-NPs and C6-BSA-PL-NPs by mouse macrophages Raw264.7. As shown in Figure 6, the fluorescent signal of C6 in cells becomes from very weak at the lowest NPs concentration to relatively strong at the highest NPs concentration, and there is no difference between C6-PL-NPs and C6-BSA-PL-NPs. The detailed amount of C6 phagocytosed by macrophages is shown in Figure 7. Consistent with the fluorescent images shown above, both C6-PL-NPs and C6-BSA-PL-NPs present a very low phagocytosis rate at low NPs concentrations and the phagocytosis is concentration dependent. This result indicates that PL-NPs are nearly not recognized by macrophages at the NPs concentration lower than 2.5 μg/mL, probably due to the fact that phospholipid is the main component of cell membrane and to its intrinsic antiadhesion property. Meanwhile, the incorporated BSA has no influence on the phagocytosis of PL-NPs. This is a critical property for long-circulation NPs. It will be ineffective for long circulation if a large amount of particles are easily recognized and phagocytosed by macrophages after administration, no matter how stable they are.

In Vitro Cytotoxicity. The cytotoxicity of PL-NPs and BSA-PL-NPs was tested using the real-time cell analysis system (RTCA, xCELLigence DP), in which the cell viability was presented as the cell index. As shown in Figure 8A, the cell index increases a little within the first few hours after exposure to PL-NPs, followed by a slow decrease, and a similar trend is

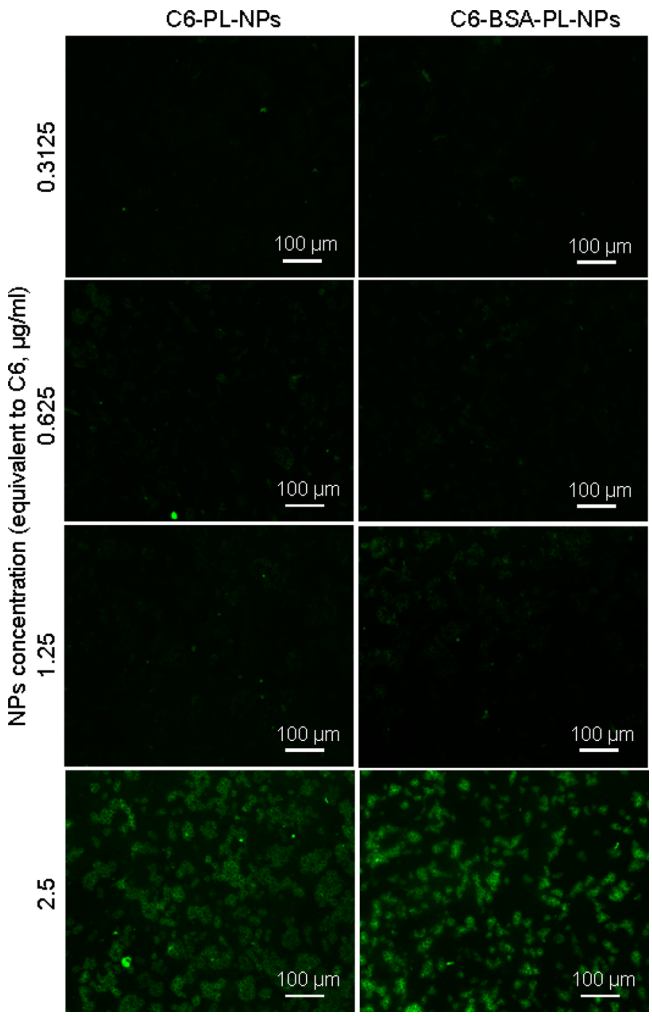

Figure 6. Fluorescent micrographs of mouse macrophages Raw264.7 exposed to different concentrations of C6-PL-NPs and C6-BSA-PL-NPs for 1 h. Scale bar: 100 μm.

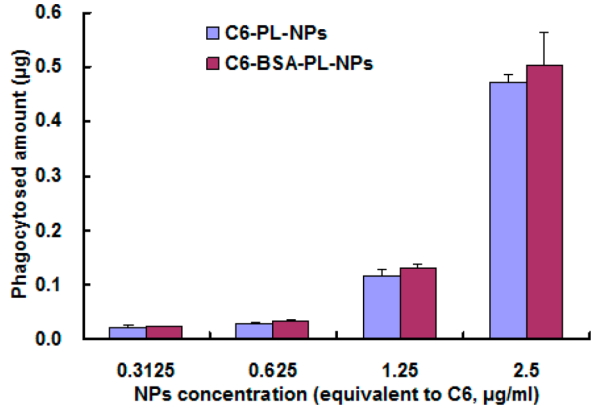

Figure 7. Phagocytosis amount of C6-PL-NPs and C6-BSA-PL-NPs with different concentrations after incubation with mouse macrophages Raw264.7 for 1 h. Data are presented as mean ± s.d. ($n = 3$).

found in all concentrations of PL-NPs and also in the control. This result suggests that PL-NPs has little toxicity to mouse L929 fibroblasts and that its particle concentration has no significant effect on cytotoxicity. In contrast, however, a significant increase in proliferation is presented after the cells are exposed to BSA-PL-NPs (Figure 8B). This result is quite

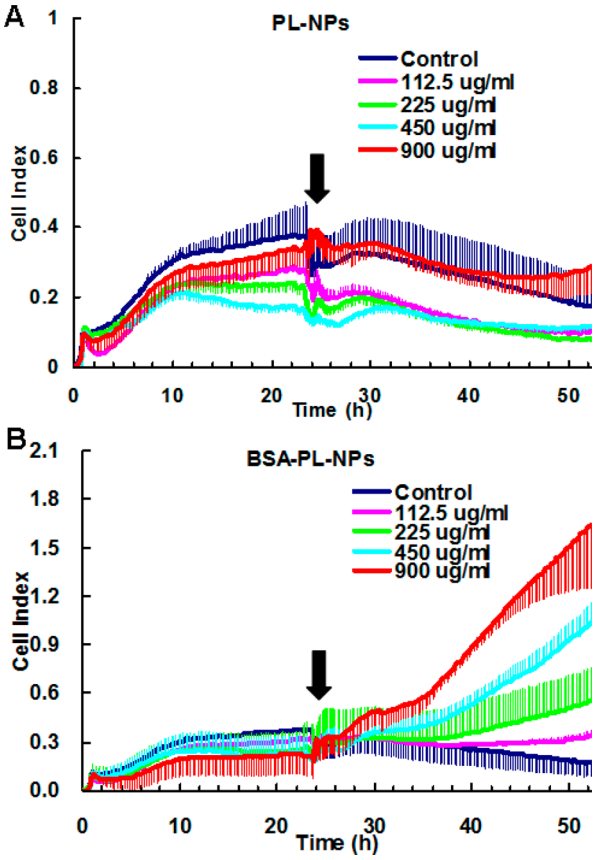

Figure 8. In vitro cytotoxicity of (A) PL-NPs and (B) BSA-PL-NPs with various particle concentrations on mouse L929 fibroblasts, detected by real-time cell analysis system (RTCA). Arrows indicate the time point NPs were added. Data are presented as mean ± s.d. (n = 3).

interesting in that BSA-PL-NPs does not show any toxicity to L929 cells but promotes its proliferation instead. Furthermore, this promoting effect is presented in an obvious concentration-dependent manner. BSA must be the origin of this change because it is the sole component difference between PL-NPs and BSA-PL-NPs. It has been reported that albumin is able to stimulate the growth of some types of cells with complicated and not fully understood mechanisms.[39,40] Our finding in this work is another evidence for the ability of albumin to promote cell proliferation. In a word, BSA-PL-NPs can be considered as a noncytotoxic drug delivery system according to the results above.

There are lots of factors that should be considered when developing NPs-based long-circulation drug delivery systems, including proteins adsorption (opsonization), drug release rate, structural and metabolic stability of nanoparticles system and the amount and speed of nanoparticles phagocytosed by macrophages. Accordingly, an ideal nanoparticles system for long-term drug delivery should address all the issues above. In this present work, we developed the albumin−phospholipid nanocomplex system (BSA-PL-NPs) that combined the antiadhesion property of phospholipids and the stabilization functions of albumin. We found that some incorporated BSA molecules were fixed on the inner surface of NPs via the hydrophobic effects between the fatty acid chain of phospholipid and hydrophobic domain of BSA, and the others were located in the core area of NPs. Such special configuration allows BSA-PL-NPs to not only maintain the antiadsorption and low phagocytosis properties but also possess slow drug release and enhanced nanostructure stability. In another word, BSA is a functional stabilizer for PL-NPs. Therefore, BSA-PL-NPs have great potential to be developed as a long-circulation drug delivery system. It should be noted that BSA is a type of albumin that can only be used for research work and cannot be used for human applications. Human serum albumin is the one appropriate for product development and practical use.

CONCLUSION

In this present work, we developed a nanocomplex drug delivery system, namely BSA−phospholipid nanoparticles (BSA-PL-NPs), in which BSA was incorporated as a functional stabilizer. Our findings showed that some BSA molecules were fixed on the inner surface of NPs via the hydrophobic effects and the others were located in the core area. It is the first time the special configuration of a nanocomplex is reported. Although further efforts investigating the in vivo behavior of the nanocomplex with encapsulating a real drug are needed to support its great applications for long-term drug delivery, its properties including antiadsorption, low phagocytosis, slow drug release, enhanced nanostructure stability and nontoxicity render it great possibility to achieve that goal. In addition, the ready availability and nontoxicity of phospholipids and albumin offer this system a great promise for rapid translation.

AUTHOR INFORMATION

Corresponding Author

*Y.-F. Lin: Tel.: +86 28 85503487. Fax: +86 28 85503487. E-mail: yunfenglin@scu.edu.cn.

Author Contributions

§Qiang Peng and Xue-Qin Wei contributed equally to this work.

Notes

The authors declare no competing financial interest.

ACKNOWLEDGMENTS

This work was funded by National Natural Science Foundation of China (31170929, 81201211), Funding of Sichuan Province Youth Science and Technology Innovation Team (2014TD010) and Funding of State Key Laboratory of Oral Diseases (SKLOD201405).

REFERENCES

(1) Tenne, R. Inorganic Nanotubes and Fullerene-like Nanoparticles. *Nat. Nanotechnol.* **2006**, *1*, 103−111.

(2) Barakat, N. S. Magnetically Modulated Nanosystems: A Unique Drug-Delivery Platform. *Nanomedicine (London, U. K.)* **2009**, *4*, 799−812.

(3) Gautam, M.; Verma, M.; Misra, G. Structural and Optical Properties of ZnO Nanocrystals. *J. Biomed. Nanotechnol.* **2011**, *7*, 161−162.

(4) Peng, Q.; Zhang, Z. R.; Gong, T.; Chen, G. Q.; Sun, X. A Rapid-Acting, Long-Acting Insulin Formulation Based on a Phospholipid Complex Loaded PHBHHx Nanoparticles. *Biomaterials* **2012**, *33*, 1583−1588.

(5) He, B.; Lin, P.; Jia, Z.; Du, W.; Qu, W.; Yuan, L.; Dai, W.; Zhang, H.; Wang, X.; Wang, J.; Zhang, X.; Zhang, Q. The Transport Mechanisms of Polymer Nanoparticles in Caco-2 Epithelial Cells. *Biomaterials* **2013**, *34*, 6082−6098.

(6) Zhang, Z.; Mei, L.; Feng, S. S. Paclitaxel Drug Delivery Systems. *Expert Opin. Drug Delivery* **2013**, *10*, 325−340.

(7) Gao, L. Y.; Liu, X. Y.; Chen, C. J.; Wang, J. C.; Feng, Q.; Yu, M. Z.; Ma, X. F.; Pei, X. W.; Niu, Y. J.; Qiu, C.; Pang, W. H.; Zhang, Q.

Core-Shell Type Lipid/rPAA-Chol Polymer Hybrid Nanoparticles for In Vivo siRNA Delivery. *Biomaterials* **2014**, *35*, 2066−2078.
(8) Shen, M.; Huang, Y.; Han, L.; Qin, J.; Fang, X.; Wang, J.; Yang, V. C. Multifunctional Drug Delivery System for Targeting Tumor and Its Acidic Microenvironment. *J. Controlled Release* **2012**, *161*, 884−892.
(9) Lalatsa, A.; Schatzlein, A. G.; Mazza, M.; Le, T. B.; Uchegbu, I. F. Amphiphilic Poly(L-amino acids) - New Materials for Drug Delivery. *J. Controlled Release* **2012**, *161*, 523−36.
(10) Wang, B.; Galliford, C. V.; Low, P. S. Guiding Principles in the Design of Ligand-Targeted Nanomedicines. *Nanomedicine (London, U. K.)* **2014**, *9*, 313−330.
(11) Mahmoudi, M.; Lynch, I.; Ejtehadi, M. R.; Monopoli, M. P.; Bombelli, F. B.; Laurent, S. Protein-Nanoparticle Interactions: Opportunities and Challenges. *Chem. Rev.* **2011**, *111*, 5610−5637.
(12) Walkey, C. D.; Chan, W. C. Understanding and Controlling the Interaction of Nanomaterials with Proteins in a Physiological Environment. *Chem. Soc. Rev.* **2012**, *41*, 2780−2799.
(13) Peng, Q.; Zhang, S.; Yang, Q.; Zhang, T.; Wei, X. Q.; Jiang, L.; Zhang, C. L.; Chen, Q. M.; Zhang, Z. R.; Lin, Y. F. Preformed Albumin Corona, A Protective Coating for Nanoparticles Based Drug Delivery System. *Biomaterials* **2013**, *34*, 8521−8530.
(14) Wang, F.; Yu, L.; Monopoli, M. P.; Sandin, P.; Mahon, E.; Salvati, A.; Dawson, K. A. The Biomolecular Corona Is Retained During Nanoparticle Uptake and Protects the Cells from the Damage Induced by Cationic Nanoparticles until Degraded in the Lysosomes. *J. Nanomed. Nanotechnol.* **2013**, *9*, 1159−1168.
(15) Salvati, A.; Pitek, A. S.; Monopoli, M. P.; Prapainop, K.; Bombelli, F. B.; Hristov, D. R.; Kelly, P. M.; Aberg, C.; Mahon, E.; Dawson, K. A. Transferrin-Functionalized Nanoparticles Lose Their Targeting Capabilities When a Biomolecule Corona Adsorbs on the Surface. *Nat. Nanotechnol.* **2013**, *8*, 137−143.
(16) Walczyk, D.; Bombelli, F. B.; Monopoli, M. P.; Lynch, I.; Dawson, K. A. What the Cell "Sees" in Bionanoscience. *J. Am. Chem. Soc.* **2010**, *132*, 5761−5768.
(17) Monopoli, M. P.; Walczyk, D.; Campbell, A.; Elia, G.; Lynch, I.; Bombelli, F. B.; Dawson, K. A. Physical-Chemical Aspects of Protein Corona: Relevance to In Vitro and In Vivo Biological Impacts of Nanoparticles. *J. Am. Chem. Soc.* **2011**, *133*, 2525−34.
(18) Ishida, T.; Ichihara, M.; Wang, X.; Kiwada, H. Spleen Plays an Important Role in the Induction of Accelerated Blood Clearance of PEGylated Liposomes. *J. Controlled Release* **2006**, *115*, 243−250.
(19) Perry, J. L.; Reuter, K. G.; Kai, M. P.; Herlihy, K. P.; Jones, S. W.; Luft, J. C.; Napier, M.; Bear, J. E.; Desimone, J. M. Pegylated PRINT Nanoparticles: The Impact of PEG Density on Protein Binding, Macrophage Association, Biodistribution, and Pharmacokinetics. *Nano Lett.* **2012**, *12*, 5304−5310.
(20) Knop, K.; Hoogenboom, R.; Fischer, D.; Schubert, U. S. Poly(ethylene glycol) in Drug Delivery: Pros and Cons as Well as Potential Alternatives. *Angew. Chem., Int. Ed.* **2010**, *49*, 6288−6308.
(21) Rojnik, M.; Kocbek, P.; Moret, F.; Compagnin, C.; Celotti, L.; Bovis, M. J.; Woodhams, J. H.; Macrobert, A. J.; Scheglmann, D.; Helfrich, W.; Verkaik, M. J.; Papini, E.; Reddi, E.; Kos, J. In Vitro and In Vivo Characterization of Temoporfin-Loaded PEGylated PLGA Nanoparticles for Use in Photodynamic Therapy. *Nanomedicine (London, U. K.)* **2012**, *7*, 663−77.
(22) Matsuno, R.; Ishihara, K. Integrated Functional Nanocolloids Covered with Artificial Cell Membranes for Biomedical Applications. *Nano Today* **2011**, *6*, 61−74.
(23) Weingart, J.; Vabbilisetty, P.; Sun, X.-L. Membrane Mimetic Surface Functionalization of Nanoparticles: Methods and Applications. *Adv. Colloid Interface Sci.* **2013**, *197−198*, 68−84.
(24) Gong, Y. K.; Winnik, F. M. Strategies in Biomimetic Surface Engineering of Nanoparticles for Biomedical Applications. *Nanoscale* **2012**, *4*, 360−368.
(25) Peng, Q.; Gong, T.; Zuo, J.; Liu, J.; Zhao, D.; Zhang, Z. Enhanced Oral Bioavailability of Salvianolic Acid B by Phospholipid Complex Loaded Nanoparticles. *Pharmazie* **2008**, *63*, 661−666.
(26) Peng, Q.; Zhang, Z. R.; Sun, X.; Zuo, J.; Zhao, D.; Gong, T. Mechanisms of Phospholipid Complex Loaded Nanoparticles Enhancing the Oral Bioavailability. *Mol. Pharmaceutics* **2010**, *7*, 565−75.
(27) Choi, S. Y.; Kim, Y. S.; Seo, Y. J.; Yang, J.; Choi, K. S. Gas-filled Phospholipid Nanoparticles Conjugated with Gadolinium Play a Role as a Potential Theragnostics for MR-Guided HIFU Ablation. *PLoS One* **2012**, *7*, E34333.
(28) Kratz, F. Albumin as a Drug Carrier: Design of Prodrugs, Drug Conjugates and Nanoparticles. *J. Controlled Release* **2008**, *132*, 171−183.
(29) Baek, M. S.; Yu, R. Z.; Gaus, H.; Grundy, J. S.; Geary, R. S. In Vitro Metabolic Stabilities and Metabolism of 2′-O-(Methoxyethyl) Partially Modified Phosphorothioate Antisense Oligonucleotides in Preincubated Rat or Human Whole Liver Homogenates. *Oligonucleotides* **2010**, *20*, 309−316.
(30) Moe, B.; Gabos, S.; Li, X. F. Real-Time Cell-Microelectronic Sensing of Nanoparticle-Induced Cytotoxic Effects. *Anal. Chim. Acta* **2013**, *789*, 83−90.
(31) Garcia, S. N.; Gutierrez, L.; Mcnulty, A. Real-Time Cellular Analysis as a Novel Approach for In Vitro Cytotoxicity Testing of Medical Device Extracts. *J. Biomed. Mater. Res., Part A* **2013**, *101*, 2097−2106.
(32) Sindhu, R.; Tiwari, A. K.; Mishra, L. C.; Husain, M. M. Spectroscopic Interaction of a Coumarin Derivative with Bovine Serum Albumin. *Cancer Biother. Radiopharm.* **2012**, *27*, 452−456.
(33) Wei, K.; Peng, X.; Zou, F. Folate-Decorated PEG-PLGA Nanoparticles with Silica Shells for Capecitabine Controlled and Targeted Delivery. *Int. J. Pharm.* **2014**, *464*, 225−233.
(34) Kumar, V.; Kumari, A.; Kumar, D.; Yadav, S. K. Biosurfactant Stabilized Anticancer Biomolecule-loaded Poly (D,L-Lactide) Nanoparticles. *Colloids Surf., B* **2014**, *117*, 505−511.
(35) Bhattacharyya, S.; Wang, H.; Ducheyne, P. Polymer-coated Mesoporous Silica Nanoparticles for the Controlled Release of Macromolecules. *Acta Biomater.* **2012**, *8*, 3429−3435.
(36) Chang, L. C.; Cheng, C. J.; Tsai, T. H.; Liu, C. W.; Tsai, T. R. Optimization of Rate-Controlled 17beta-Estradiol Nanoparticles for Cerebral Ischemia Therapy. *J. Biomed. Nanotechnol.* **2013**, *9*, 1724−1735.
(37) Salvati, A.; Åberg, C.; dos Santos, T.; Varela, J.; Pinto, P.; Lynch, I.; Dawson, K. A. Experimental and Theoretical Comparison of Intracellular Import of Polymeric Nanoparticles and Small Molecules: Toward Models of Uptake Kinetics. *J. Nanomed. Nanotechnol.* **2011**, *7*, 818−826.
(38) Lesniak, A.; Salvati, A.; Santos-Martinez, M. J.; Radomski, M. W.; Dawson, K. A.; Åberg, C. Nanoparticle Adhesion to the Cell Membrane and Its Effect on Nanoparticle Uptake Efficiency. *J. Am. Chem. Soc.* **2013**, *135*, 1438−1444.
(39) Ashman, N.; Harwood, S. M.; Kieswich, J.; Allen, D. A.; Roberts, N. B.; Mendes-Ribeiro, A. C.; Yaqoob, M. M. Albumin Stimulates Cell Growth, L-Arginine Transport, and Metabolism to Polyamines in Human Proximal Tubular Cells. *Kidney Int.* **2005**, *67*, 1878−1889.
(40) Francis, G. L. Albumin and Mammalian Cell Culture: Implications for Biotechnology Applications. *Cytotechnology* **2010**, *62*, 1−16.